Geosynthetics - 7th ICG - Delmas, Gourc & Girard (eds) © 2002 Swets & Zeitlinger, Lisse ISBN 90 5809 523 1

Time-dependant deformation of geosynthetics and geosynthetic-reinforced soil structures

D.HIRAKAWA, T.UCHIMURA, Y.SHIBATA and F.TATSUOKA
The University of Tokyo, Japan

ABSTRACT: A series of special tensile tests of a geogrid and a special model test of geogrid-reinforced gravel structure were performed to evaluate their viscous deformation characteristics. It is shown that the isochronous model, according to which the stress is a function of instantaneous strain and elapsed time, is not able to explain the test results, in particular the stress-strain behavior after loading is restarted at a constant strain rate following creep or stress relaxation stage. It is argued that the widely accepted concept, stemming from the isochronous model, that the creep is a degradation phenomenon thus the design strength should be decreased with the design life time is not correct. A non-linear three-component model is proposed to simulate the elasto-viscoplastic deformation property of geosynthetics. It is shown that this new rheology model can simulate very well the results from the present study.

1 INTRODUCTION

Permanent geosynthetic-reinforced soil (GRS) structures, including soil retaining walls and bridge abutments, are increasingly being used due to their high cost-effectiveness (e.g., Tatsuoka et al. 1997). As the tensile deformation and strength property of polymer geosynthetics is known to be more-or-less viscous (e.g., Bathurst and Cai 1994), accurate evaluation and interpretation of the viscous aspects of tensile stress-strain behaviour of geosynthetics, is of great significance in particular for; 1) relevant evaluation of the design strength of geosynthetic reinforcement for a given life time; and 2) accurate prediction of creep deformation of GRS structures. It seems however that the basic mechanism of time-dependent strength and deformation characteristics of geosynthetics is not yet well understood.

In view of the above, a series of special tensile tests of a typical geosynthetic and a special loading test on a model of GRS structure were performed in the present study.

2 CURRENT DESIGN CONCEPT

It is the currently design practice to reduce by using a relatively large creep reduction factor, based on the creep-rupture curve, the peak strength obtained from tensile rupture tests at a relatively high strain rate, say 1.0 %/sec (i.e., the unfactored strength) to obtain the design tensile rupture strength at a specified design life time (Figure 1). However, some existing data show that the ultimate tensile strength of some typical geosynthetics obtained from loading tests performed after long-term creep tests was not particularly smaller than the value obtained from similar tests performed at the same strain rate before the creep test (e.g., Paulson & Bernardi 1997; Hirai et al. 2000). The present practice illustrated in Figure 1 could be highly conservative and misleading (e.g., Greenwood 1997 & 1998; Greenwood et al. 2001).

The use of a creep reduction factor is implicitly based on the a concept that creep is a degradation phenomenon for the tensile rupture strength of geosynthetics. This concept is seemingly linked to the description of time-dependent strength and deformation characteristics of geosynthetics by the isochronous concept. According to the isochronous concept, the current stress of a given geosynthetic reinforcement is a unique function of the instantaneous strain that has developed and the time that has elapsed since the start of loading. That is, as illustrated in Figure 2, the stress-strain curve by monotonic loading at a certain constant strain rate continuously traverses, from the left to the right, given relationships between the load (or stress) and the strain defined for increasing fixed elapsed times (i.e., t= $t_1 < t_2 < t_3 < t_4 \ldots$). The behaviour during a creep stage and a stress relaxation stage also follows this rule, while the same state ***X*** is reached at the same elapsed time for different stress histories. When loading is restarted from point ***X*** after a creep stage at the original strain rate, the stress-strain curve becomes like the one denoted as ***XA***, bound for point ***A***. As curve ***XA*** is located consistently lower than the isochronous curve for the elapsed time at the end of the creep stage ($t = t_5$), the ultimate rupture strength should decrease because of this creep history and the ultimate strength decreases more with the time duration at the creep stage.

However, as argued by Tatsuoka et al. (2001a) and demonstrated in this paper, the stress-strain behaviour after loading is restarted at the original strain rate from point ***X*** rejoins the original curve (bound for point ***B***), maintaining the original ultimate

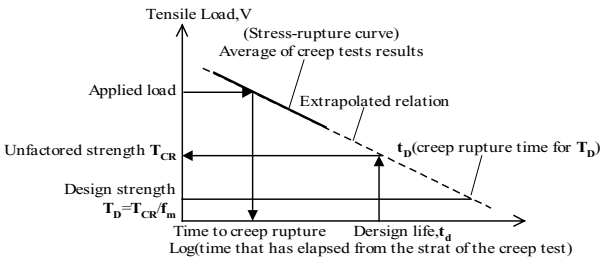

Figure 1. Current design practice to determine the design tensile strength geotextile of geogrid based on the creep results (after Greenwood, 1997,1998)

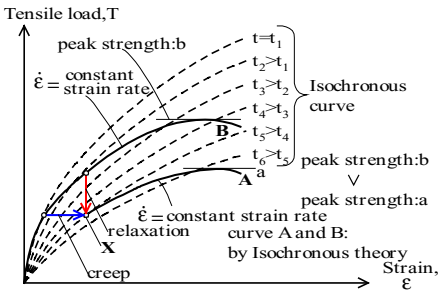

Figure 2. Response of geosynthetic reinforcement according to the isochronous theory

rupture strength, indicating that the isochronous concept is incorrect. The isochronous concept is known to have serious limitations also in predicting the strength and deformation characteristics of geomaterials (i.e., soils and rocks; Tatsuoka et al. 2000).

3 TEST METHOD AND TEST MATERIAL

A polyester geogrid having an aperture of 9 mm in the longitudinal and transversal directions, coated with polyethylene for protection (*type; KTG-4000, Taiyo Kogyo Co., Japan*) was used. The ultimate strength by tensile tests (at a strain rate of 1 %/min) is 39.2 kN/m with a strain at failure less than 22 % in both longitudinal and transversal directions. This is one of relatively weak reinforcement types among those used for prototype structures, while this is being used in model tests in the authors' laboratory.

Figure 3a shows the newly designed tensile loading apparatus. The specimen was 5 cm wide having 5 transversal members. The total length was about 90 cm, while the initial length of the unconfined part was 24 cm with an initial gauge length of about 6 cm for local axial strain measurements. The gripping device consists of a steel cylinder, to which a specimen was wrapped-around, and a small-diameter steel bar, by which the end of the specimen was fixed to a groove made in the steel cylinder. In all the tests using this device, tensile rupture took place in between the gripping devices, as seen in Figure 3b.

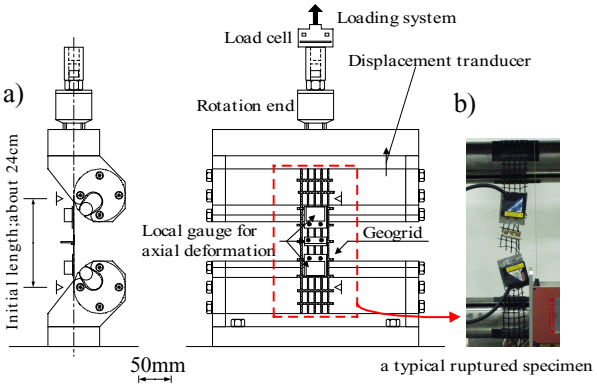

Figure 3. a) Set up of the tensile tests, and b) a typical ruptured specimen

The loading system had a capacity of 50 kN, of precision gear type with practically no backlash when the loading direction is reversed. By using this loading system, it becomes possible; a) to smoothly switch between strain and stress control loading phases and between a creep or stress relaxation stage and constant strain rate loading or unloading; b) to change the strain rate, stepwise or gradually, by a factor of up to 3000; and c) to apply very small amplitude unload/reload cycles during otherwise constant strain rate loading (Santucci de Magistris et al., 1999). Axial strains at the central part of specimen were measured locally by using a pair of laser displacement sensors. The temperature in the laboratory was not very constant within 23±2 degrees Celsius.

4 TEST RESULTS AND DISCUSSIONS

Figure 4a shows the relationships between the tensile load per unit width and the local axial tensile strain at constant strain rates that were different by a factor of up to 2,000. Significant effects of loading rate may be seen. As it is not possible to examine whether the isochronous model is relevant only based on these test results, a special tensile test was performed (Figure 5), in which creep and relaxation stages were included during otherwise monotonic loading. In Figure 5, some of the test results presented in Figure 4 are also presented. The following trends of behaviour may be noted from Figure 5.

1) The geogrid shows a very stiffness, close to the elastic value, immediately after; a) loading is restarted at a constant strain rate following creep and stress relaxation stages; and b) a step increase in the strain rate. Subsequently, the load-strain relationship exhibits clear yielding and noticeable stress over-shooting before rejoining the original one that would be obtained by continuous monotonic loading at the constant strain rate that is the same as the one after the restart of loading.
2) The behavior that is opposite to the above takes place immediately after the strain rate is decreased stepwise.

The elastic stiffness k_{eq} obtained from small unload/reload cycles is essentially independent of strain rate, although it is a function of stress level (Figure 6a). The peak strength of the geogrid increases with the strain rate at failure, not controlled by the time that has been elapsed (Figure 6b).

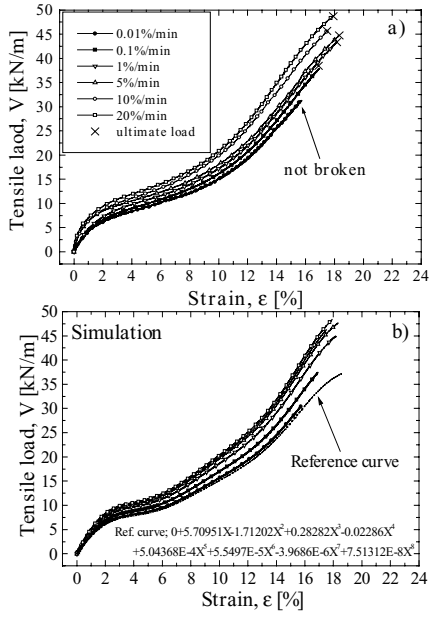

Figure 4. Dependency of tensile-elongation property on strain; a) measured; and b) simulated

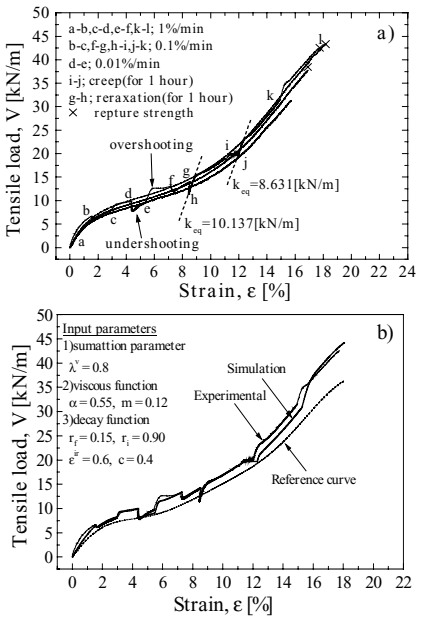

Figure 5. Viscous effects on the deformation characteristics; a) measured and b) simulated

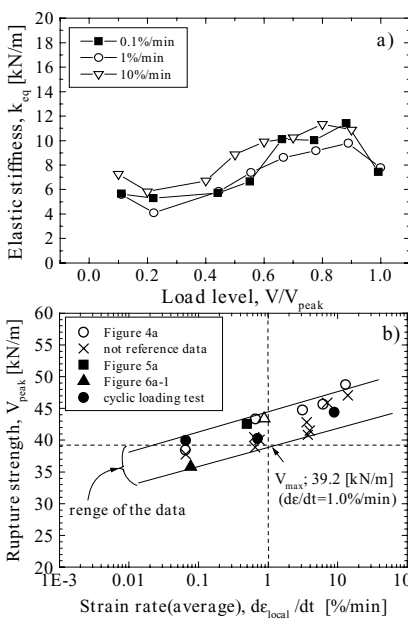

Figure 6. a) Relationship between elastic stiffness and load level, and b) strain rate dependency of rupture strength

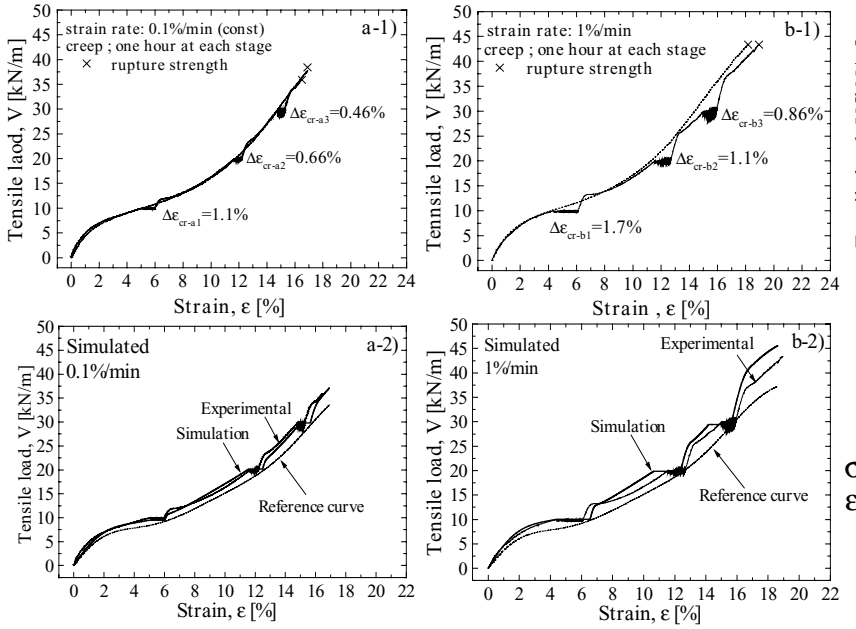

Figure 7. Results from tests with creep stages; strain rate=; a-1) 0.1%/min (measured), a-2) simulated; and b-1) 1%/min (measured), b-2) simulated

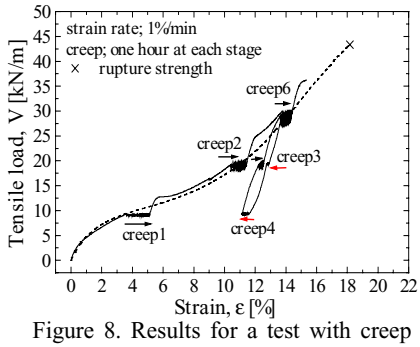

Figure 8. Results for a test with creep stages; with a large amplitude unloading/reload cycle

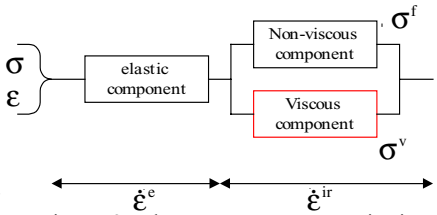

Figure 9. Three-component constitutive model (Tatsuoka et al.; 2001; Di Benedetto et al.2001)

For confirmation, multiple stage creep tests also were performed, each lasting for one hour, at 25 %, 50 % and 75 % of the average ultimate strength, equal to 39.2 kN/m (at an axial strain rate of 1 %/min) during otherwise monotonic loading at different constant strain rates, 0.1 %/min and 1.0 %/min (7a-1 and 7b-1). In addition to the fact 1) above, the following important trends may also be seen from Figure 7:

a) The creep strain developed for a given period at a given stress level decreases with the decrease in the strain rate at the start of creep stage.
b) The creep strain developed for a given period with the same initial strain rate decreases with the increase in the creep load level, which is opposite to the trend usually considered.

In another test, creep tests were performed during not only global loading but also global unloading and reloading (Figure 8). In addition to the fact b) above, the following may be seen:

c) The creep strain becomes negative under unloaded conditions and the amount of negative creep increases with the decrease in the stress level.
d) The creep strain during global reloading becomes positive again, while the creep strain is much smaller than the one observed at the creep stage during the primary loading.

The data presented above indicate that the deformation and the ultimate rupture strength of geosynthetics is essentially a function of the instantaneous irreversible strain rate, while independent of the time that has elapsed since the start of loading. This fact means that creep is not a degradation phenomenon, like weathering and degradation chemical process. Therefore, it is not necessary to introduce a correction factor for creep when evaluating the design rupture strength, but it should be defined for a design strain rate. It is also seen that the isochronous model seriously underestimates the tensile rupture strength of geosynthetic reinforcement when subjected to relatively fast loading, such as seismic loading, after having been subjected to sustained load for a long duration.

It has been shown that the three-component model, which is one of the non-linear rheology models, can simulate very well the stress-strain-time behaviour of geomaterials subjected to arbitrary stress histories (Fig. 8; Di Benedetto et al., 2001; Tatsuoka et al., 2001b). According to this model, the stress is decomposed as follows for the monotonic loading case:

$$\sigma = \sigma^{f}\left(\varepsilon^{ir}\right) + \sigma^{v}\left(\varepsilon^{ir}, \dot{\varepsilon}^{ir}, h_s\right) \quad (1)$$

where $\sigma^{f}(\varepsilon^{ir})$ is the inviscid stress component that is a unique function of the instantaneous irreversible strain ε^{ir}, while $\sigma^{v}\left(\varepsilon^{ir}, \dot{\varepsilon}^{ir}, h_s\right)$ is the viscous stress that is a function of ε^{ir}, its rate $\dot{\varepsilon}^{ir}$ and the stress history parameter h_s. To simulate the whole of the behaviour described above and others that would be observed for more general loading histories, the following specific type of $\sigma^{v}\left(\varepsilon^{ir}, \dot{\varepsilon}^{ir}, h_s\right)$ was considered:

$$\sigma^{v}(\varepsilon^{ir}, \dot{\varepsilon}^{ir}, h_s) = \lambda^{v} \cdot \sigma^{v}_{iso}(\varepsilon^{ir}, \dot{\varepsilon}^{ir}) + (1-\lambda^{v}) \cdot \sigma^{v}_{TESRA}(\varepsilon^{ir}, \dot{\varepsilon}^{ir}, h_s) \quad (2)$$

here λ^{v} is the parameter, which is obtained experimentally; $\sigma^{v}_{iso}(\varepsilon^{ir}, \dot{\varepsilon}^{ir})$ is the viscous stress component that is a unique function of the instantaneous values of ε^{ir} and $\dot{\varepsilon}^{ir}$ (called the isotach component), which is assumed as follows based on the test results presented above:

$$\sigma^{v}_{iso}\left(\varepsilon^{ir}, \dot{\varepsilon}^{ir}\right) = \sigma^{f}\left(\varepsilon^{ir}\right) \cdot g_{v}\left(\dot{\varepsilon}^{ir}\right) \quad (3)$$

where $g_{v}(\dot{\varepsilon}^{ir})$ is the viscous function, which is given as:

$$g_{v}(\dot{\varepsilon}^{ir}) = \alpha \cdot [1 - \exp\{1 - (\frac{\dot{\varepsilon}^{ir}}{\dot{\varepsilon}^{ir}_{r}} + 1)^{m}\}] \ (\geq 0) \quad (4)$$

where α, m and $\dot{\varepsilon}^{ir}_{r}$ are the positive material constants.

The viscous stress component $\sigma^{v}_{TESRA}(\varepsilon^{ir}, \dot{\varepsilon}^{ir}, h_s)$ in Eq. 2 is the TESRA (Temporary Effects of Strain Rate and strain Acceleration) component, given as:

$$\sigma^{v}_{TESRA} = \int_{\tau=\varepsilon^{ir}_{1}}^{\varepsilon^{ir}} \left[d\left\{\sigma^{f}(\varepsilon^{ir}) \cdot g_{v}(\dot{\varepsilon}^{ir})\right\} \right]_{(\tau)} \cdot \left\{ r(\varepsilon^{ir}) \right\}^{(\varepsilon^{ir} - \tau)} \quad (5)$$

where τ is the irreversible strain at which the viscous stress increment $d\left\{\sigma^{f}(\varepsilon^{ir}) \cdot g_{v}(\dot{\varepsilon}^{ir})\right\}$ takes place; $\left\{ r(\varepsilon^{ir}) \right\}^{(\varepsilon^{ir} - \tau)}$ is the decay function for the viscous stress component σ^{v}_{TESRA}, decreasing from the initial value, unity, with the irreversible strain difference $\varepsilon^{ir} - \tau$; and $r(\varepsilon^{ir})$ is the parameter that is a function of ε^{ir}, given as:

$$r(\varepsilon^{ir}) = r_i = 1.0 \qquad \text{at } \varepsilon^{ir} = 0 \quad (6a)$$

$$r(\varepsilon^{ir}) = \frac{r_i + r_f}{2} + \frac{r_i - r_f}{2} \cdot \cos\left\{ \pi \cdot \left(\frac{\varepsilon^{ir}}{c} \right)^{n} \right\} \quad \text{for } 0 \leq \varepsilon^{ir} \leq c \quad (6b)$$

$$r(\varepsilon^{ir}) = r_f \qquad \text{for } \varepsilon^{ir} \geq c \quad (6c)$$

According to this model, due to the features of the isotach viscous component, the stress-strain relationships in monotonic

loading tests at constant but different irreversible strain rate $\dot{\varepsilon}^{ir}$ are separated from each other, the separation becoming larger with ε^{ir} (Figure 4). When the irreversible strain rate $\dot{\varepsilon}^{ir}$ is changed stepwise, due to the features of the TESRA viscous component, the viscous effects become noticeable while they decay with the increase in ε^{ir} when loading at a constant strain continue (Figure 5).

Figures 4b, 5b, 7a-2 and 7b-c show the results of simulation by this model of the test results presented in this paper. The σ^{f} - ε^{ir} relationship (called the reference relation) was determined to fit to the general feature of the entire stress-strain relation, while the parameters for the viscous feature were determined to obtain the best fitting. It is seen from these figures that the proposed model can simulate rather accurately the various viscous aspects of the tested geogrid subjected to a wide range of stress histories. As the same parameters were used for all the test results, some inconsistency between the measured and simulated results may be noted due mostly to an inevitable scatter in the test results. This model can also simulate the viscous property observed during global unloading and reloading as seen from Figure 8c (Tatsuoka et al., 2001a), which will be reported elsewhere in the future.

5 MODEL TESTS ON GEOGRID-REINFORCED GRAVEL STRUCTURE

Figure 10 shows the result from a model test on a gravel structure reinforced with the polymer geogrid described above. The models were 60 cm-high and 35 cm by 35 cm in cross-section, simulating a bridge abutment or pier. The backfill was a well-graded gravel of crushed sandstone (D_{50}= 2.52 mm; U_c= 5.41; fines content= 0 %; e_{max}= 0.986; and e_{min}= 0.481), which was compacted by manual tamping to a relative density of 90 % in 12 sub-layers and reinforced with 12 geogrid layers with a vertical spacing of 5 cm. The periphery of each sub-layer of backfill was protected with two layers of small gravel-filled fabric bags having a diameter of about 3.5 cm. The end of each reinforcement layer was connected to the respective gravel bags. A square steel platen of 5 cm in thickness and 45 cm by 45 cm in cross-section with a weight of 282 N was placed on the crest of the reinforced backfill. Vertical load was applied using a controlled history of strain rate with several step changes in the strain rate and two creep stages during otherwise monotonic loading at different constant strain rates, similar to the test described in Figure 5. It is seen that the dependency on loading rate of the model deformation is noticeable showing viscous aspect that is essentially the same with that of the geogrid alone. This result is not surprising, because the three-component rheology model can also simulate very well the viscous aspect of the deformation of the gravel alone (Tatsuoka et al. 2001a).

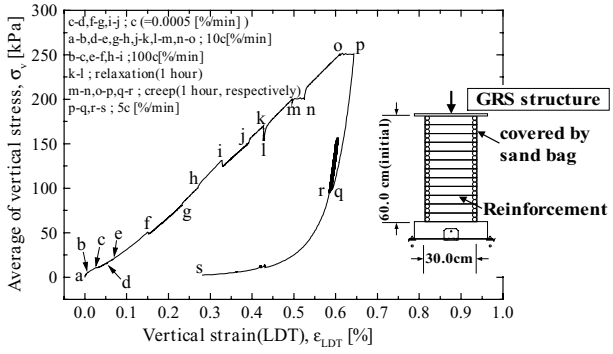

Figure 10. Behaviour of a model of geogrid-reinforced gravel structure during a creep stage and cyclic loading unloading condition

6 CONCLUSIONS

The following conclusions can be derived from the present study:

1) The tested geogrid became very stiff when loading was restarted at a constant strain rate after a creep stage. After exhibiting a clear yielding and a noticeable stress overshooting, the stress-strain relation rejoined the original one that would have been obtained by continuous loading. The ultimate strength of the geogrid was a function of the strain rate at failure, not affected by creep histories at intermediate pre-peak stages.
2) Time is not the basic parameter controlling the time-dependent deformation of geosynthetic, showing that the isochronous concept is not relevant and creep is not a degradation phenomenon.
3) A non-linear three-component rheology model that was developed taking into account the fact that the stress-strain property of the tested geogrid be a function of the instantaneous irreversible strain rate and the stress history could successfully simulate the obtained test results.
4) A geogrid-reinforced gravel structure model also exhibited noticeable viscous deformation having features that were very similar to those observed with the geogrid alone and the gravel alone.

REFERENCES

1) Bathurst,R.J. and Cai,Z. (1994), In-isolation cyclic load-extension behavior of two geogrid, *Geosynthetics International*, Vol.1, No.1, pp.3-17
2) Di Benedetto,H., Tatsuoka,F. and Ishihara,M. (2001), Time-dependant deformation characteristics of sand and their constitutive modeling, *Soils and Foundations* (to be published)
3) Greenwood,J.H. (1997), Residual strength: An alternative to stress-rupture for earth resinforcement design, *Proc. of the International Symposium of Earth Reinforcement, IS-Kyushu* (Ochiai et al. eds.), Balkema, pp.1081-1083
4) Greenwood,J.H. (1998), Designing to residual strength of geogsynthetics instead of stress-rupture, *Geosynthetics International*, Vol.4, No.1, pp.1-10
5) Greenwood,J.H., Johns,C.J.F.P. and Tatsuoka,F (2001), Residual strength and its application to design of reinforced soil in seismic areas, *Proc. of the International Symposium of Earth Reinforcement, IS-Kyushu* (Ochiai et al. eds.), Balkema, pp.37-42
6) Hirai,T. and Yatsu,A. (2000), Evaluation method about tensile strength of geogrid to use for dynamic design, *Journal of Geosynthetics Engineering, Japan Chapter of the International Geosynthetics Society*, Vol.15, pp.205-214 (in Japanese)
7) Bernardi,M. and Paulson,J. (1997), Is creep a degradation phenomenon ?, *Mechanically Stabilized Backfill* (Wu,J.T.H eds.), Balkema, pp.329-334
8) Santucci de Magistris,F., Koseki,J., Amaya,M., Hamaya,S., Sato,T. and Tatsuoka,F. (1999), "A triaxial testing system to evaluate stress-strain behaviour of soils for wide range of strain and strain rate", *Geotechnical Testing Journal, ASTM,* Vol.22, No.1, pp.44-60.
9) Tatsuoka,F., Tateyama.M., Uchimura.T. and Koseki.J. (1997), Geosynthetics Reinforced Soil Retaining Walls as Important Permanent Structures, 1996-1997 *Mercer Lecture*, *Geosynthetics International*, Vol.4, No.2, pp.81-136
10) Tatsuoka,F., Santucci de Magistris,F., Hayano,K., Momoya,Y. and Koseki,J. (2000): "Some new aspects of time effects on the stress-strain behaviour of stiff geomaterials", Keynote Lecture, *The Geotechnics of Hard Soils – Soft Rocks, Proc. of Second Int. Conf. on Hard Soils and Soft Rocks, Napoli,* 1998 (Evamgelista and Picarelli eds.), Balkema, Vol.2, pp1285-1371.
11) Tatsuoka,F., Uchimura,T., Hayano,K., Di Benedetto,H., Koseki.J and Siddiquee,M.S.A (2001a), Time-dependant deformation characteristics of stiff geomaterials in engineering practice, *Proc. of Second International Conference on Pre-Failure Deformation Characteristics of Geomaterials*, Torino, 1999 (Jamiolkowski et al. eds.), Balkema, Vol.2, pp.1161-1250.
12) Tatsuoka,F., Ishihara,M., Di Benedetto,H. and Kuwano,R. (2001b), Time-dependent deformation characteristics of geomaterials and their simulation, *Soils and Foundations* (to be published)